

# 6

## Real-Time In Vivo Monitoring of Cellular Energy Metabolism

---

6.1	Introduction .....	137
6.2	Brief History of NADH as Natural Biomarker .....	140
6.3	Methods.....	141
	Principles and Technological Aspects of In Vivo NADH Monitoring • Direct Current Fluorometer/ Reflectometer • Time-Sharing Fluorometer/ Reflectometer • Preparation of Various Organs for Measurements • Calibration of the Monitored Signals	
6.4	Pitfalls and Remedies.....	144
	Movement-Based Artifacts • Vascular Events • Intra- and Extracellular Space Events	
6.5	Applications.....	147
	Effects of Anoxia on Brain • Effects of Adrenaline on the Small Intestine and the Brain • Effect of Oxygen Deprivation on the Heart • Responses of the Spinal Cord to Ischemia • Multiorgan Responses to Hypoxia	
6.6	Summary.....	153
	References.....	154

Avraham Mayevsky  
*Bar-Ilan University*

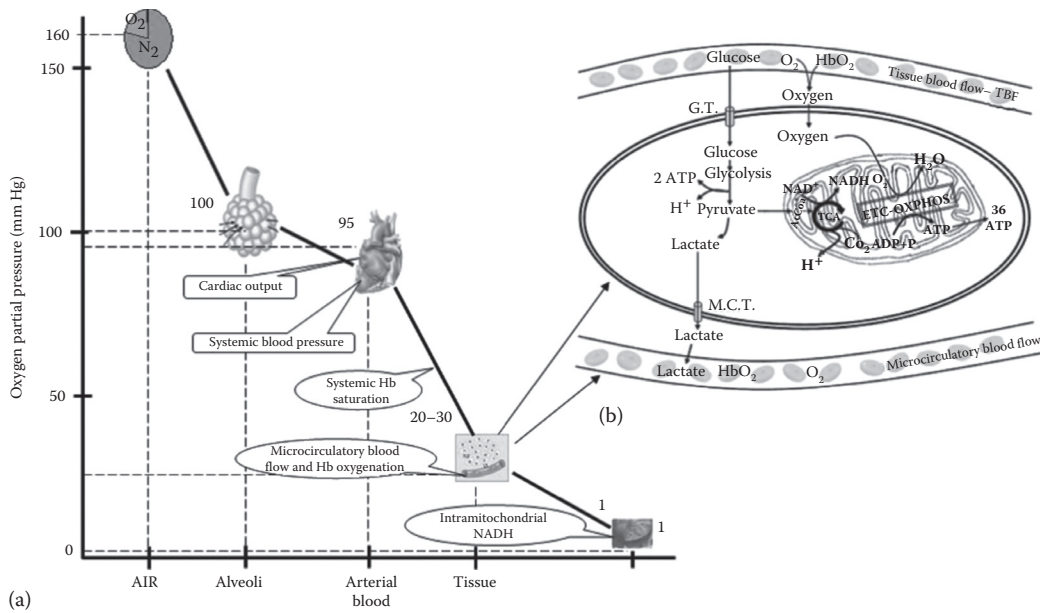
Efrat  
Barbiro-Michaely  
*Bar-Ilan University*

### 6.1 Introduction

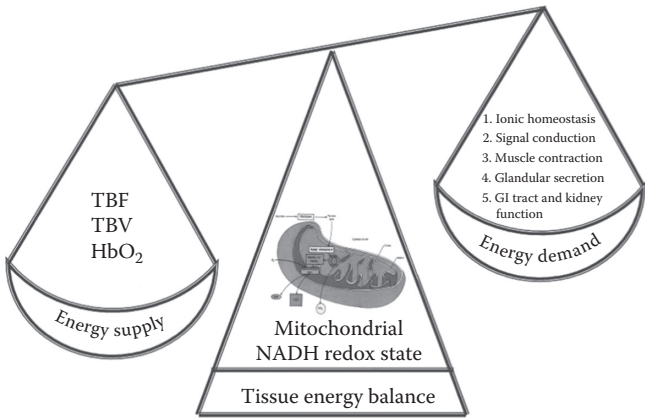
---

Tissue oxygen or energy positive balance is necessary for the required level of ATP production by mitochondria. The majority of oxygen in a mammalian organism is delivered to cells by erythrocytes: it diffuses along the partial pressure gradient from the lungs (100 mm Hg) to the bloodstream, where it combines chemically to hemoglobin (Hb) in erythrocytes and is carried by convective transport through the large vessels down to arterioles and capillaries. Smaller pressure near the mitochondria (1 mm Hg) favors oxygen diffusion from the microcirculation compartments into the cells (Figure 6.1).

Oxygen supply to the cells in all tissues is determined by the level of Hb saturation, as well as microcirculatory blood flow and volume. The demand for oxygen or energy currencies in different tissues is also dependent upon the physiological and biochemical activities in each tissue or organ (Figure 6.2). Changes in oxygen supply, oxygen demand, or both determine the oxygen balance. In normal tissues, stored energy meets the demand within a certain range. An increase in energy demand, however, will induce an increase in oxygen supply via elevating microcirculatory blood



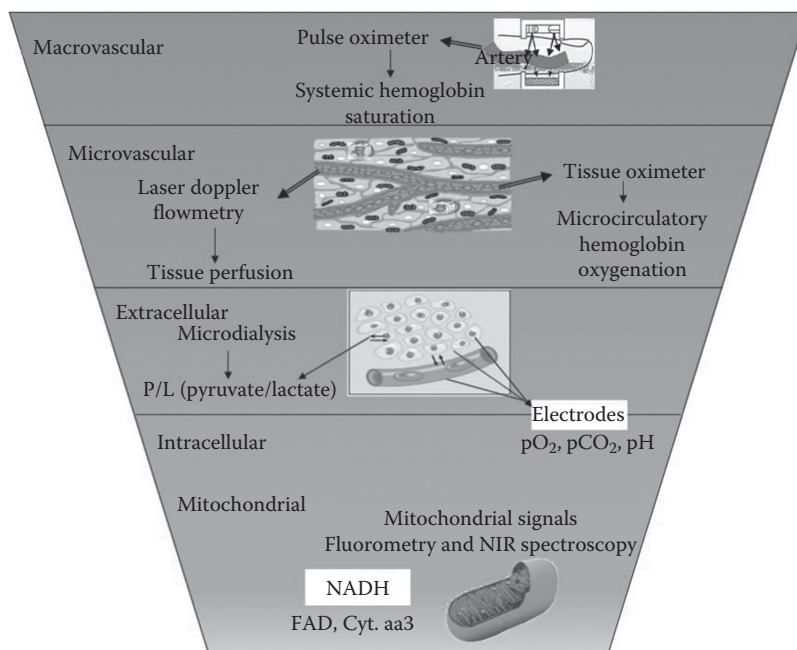
**FIGURE 6.1** (a) Oxygen gradient from its high level in the air to its very low level in the mitochondria. (b) All cells and tissues accept oxygen and substrates from the bloodstream. Oxygen is transferred in the blood by the hemo-globin. It is then diffused from the blood to the extracellular space and to the intracellular space. There it serves in the mitochondria to induce ATP.



**FIGURE 6.2** Mitochondrial NADH redox state level is a good indicator of the balance between tissue energy supply by the bloodstream, which is similar in all tissues, and tissue energy demand, which is specific to each tissue and depends on its activity.

flow, which delivers more oxygenated blood. In contrast, a decrease in oxygen supply will limit oxygen utilization and lead to the development of hypoxic damage in brain and other organs (Mayevsky and Chance 1982).

Evaluation of tissue energy metabolism *in vivo* can be carried out by monitoring various physiological parameters as shown in Figure 6.3. Given the coupling of ATP production to the availability of oxygen, and thereby to microcirculation, energy metabolism could be evaluated by the levels of



**FIGURE 6.3** Tissue oxygenation and energy state are monitored in various methods, which can be divided according to monitoring location. The pulse oximeter monitors the macrovascular bed, whereas laser Doppler flowmetry monitors the microvascular bed and so does the tissue oximeter. Mini- and microelectrodes are used for the monitoring of various chemicals in the extracellular and intracellular spaces as well as in the bloodstream. The most accurate intracellular indicator for tissue energy state in vivo is the mitochondrial NADH redox state. In other studies, flavins and cytochrome aa3 were monitored but the contamination of blood volume and oxygenation was not eliminated.

oxygen in arterioles and capillaries. Most of the current methods, for example, pulse oximeter, which is routinely used in clinics, probe oxygen content only in macrovascular compartments. However, microcirculatory blood flow and Hb oxygenation can still be monitored in arterioles and capillaries (Meirovithz et al. 2007).

Microdialysis is another approach that enables the measurement of metabolite (e.g., pyruvate and lactate) levels in the extracellular space. Such measurement can also be conducted by surface electrodes, providing with the partial pressure of oxygen ( $pO_2$ ) and carbon dioxide ( $pCO_2$ ), as well as the hydrogen ion concentration (pH). This method reflects the overall changes in  $pO_2$ ,  $pCO_2$ , and pH levels in intracellular volume, extracellular space, and the small blood vessels and does not distinguish between these compartments. The direct and most accurate approach for in vivo cellular energy metabolism evaluation is based on the optical monitoring of NADH, flavoproteins (Fp), and cytochrome aa3. Of these, only the NADH redox state allows for relatively accurate measurements: as of today, the correction of the Fp and cytochrome aa3 measurements for hemodynamic changes in blood-perfused organs in vivo is almost impossible. The level of NADH autofluorescence was also considered a good indicator for decreased oxygen availability in cellular compartments (Chance et al. 1973) under both in vitro and in vivo conditions.

In this chapter, we will discuss current methods of in vivo NADH monitoring, describe the setups and necessary calibrations, review the pitfalls and remedies, and assess the potential of this approach in the clinical diagnosis of pathologies.

## 6.2 Brief History of NADH as Natural Biomarker

Over a century of mitochondria research in relation to energy metabolism can be divided into three periods, summarized in Table 6.1 (for a review, see Mayevsky and Rogatsky, 2007). During the first period (1906–1955), NADH was discovered and its absorbance and fluorescence measurements were first performed. The second period (1956–1973) was marked by a transition from monitoring NADH in vitro (by its absorbance) to in vivo (by its fluorescence) in various organs and animal models. During the third period (1974 until today), the number of NADH monitoring methods and applications significantly expanded. This period also highlights a shift from NADH monitoring in animals to its clearance by the Federal Drugs Administration (FDA) for use in clinics.

The breakthrough in the field was achieved by the seminal work by Chance and Williams (1955), who showed for the first time that NADH can be used as an optical biomarker of energy metabolism. Under in vitro conditions, Chance and Williams defined different metabolic states of isolated mitochondria by changing the levels of ADP, substrate (energy-rich compound), and oxygen (Table 6.2). They also measured the redox state of NADH, flavoproteins, and cytochromes through the absorbance of the mitochondrial suspension. At the initial State 1, ~90% of NAD was found to be reduced. Addition of ADP to the mitochondrial suspension led to the exhaustion of the endogenous substrate and full oxidation of NADH (State 2). Under this state, the ADP was available, but the substrate became the limiting factor. Transition to State 3 with the addition of various substrates was marked by a considerable reduction of

TABLE 6.1 Milestones in the Early Period of Mitochondrial NADH Monitoring

Year	Discovery	Author(s)
1905	Involvement of adenine containing nucleotides in yeast fermentation	Harden and Young (1906)
1935	Description of the complete structure of “hydrogen-transferring coenzyme” in erythrocytes	Warburg et al.
1936	Definition of the cofactors NAD (originally denoted diphosphopyridine nucleotide [DPN]) and NADP (originally denoted triphosphopyridine nucleotide [TPN])	Warburg
1951	A shift in the absorption spectrum of NADH with alcohol dehydrogenase	Theorell and Bonnicksen
1952	Development of a rapid and sensitive spectrophotometer	Chance and Legallias
1952	Monitoring of pyridine nucleotide enzymes	Chance
1954	The first detailed study of NADH using fluorescence spectrophotometry	Duysens and Ames
1958	Measurement of NADH fluorescence in isolated mitochondria	Chance and Baltscheffsky
1959	Measurement of muscle NADH fluorescence in vitro	Chance and Jobsis
1962	In vivo monitoring of NADH fluorescence from the brain and kidney	Chance et al.
1965	Comparison between NADH fluorescence in vivo and enzymatic analysis of tissue NADH	Chance et al.
1968	Monitoring tissue reflectance in addition to NADH fluorescence	Jobsis and Stansby
1971	The first attempt to monitor the human brain during a neurosurgical procedure	Jobsis et al.
1973	The first fiber-optic-based fluorometer–reflectometer used in the brain of an awake animal	Chance et al. Mayevsky and Chance
1982	Simultaneous monitoring of NADH in vivo in four different organs in the body	Mayevsky and Chance
1985	Monitoring of brain NADH together with 31P NMR spectroscopy	Mayevsky et al.
1991	Simultaneous real-time monitoring of NADH, CBF, ECoG, and extracellular ions in experimental animals and in the neurosurgical operating room	Mayevsky et al.
1996	The multiparametric response (including NADH) to cortical spreading depression that is for the first time measured in a comatose patient	Mayevsky et al.
2000	Development of the FDA-approved “tissue spectroscope” medical device for real-time monitoring of NADH and tissue blood flow	Mayevsky et al.
2006	Monitoring of tissue vitality (NADH, TBF, and HbO <sub>2</sub> ) by a new “CitiView” device	Mayevsky et al.

**TABLE 6.2** Metabolic States of Mitochondria In Vitro and Associated Oxidation–Reduction Levels of Respiratory Enzymes

State	[O <sub>2</sub> ]	ADP Level	Substrate Level	Respiration Rate	Rate-Limiting Substance	NADH (%)
1	>0	Low	Low	Slow	ADP	~90
2	>0	High	~0	Slow	Substrate	0
3	>0	High	High	Fast	Respiratory chain	53
4	>0	Low	High	Slow	ADP	99
5	0	High	High	0	Oxygen	~100

NAD<sup>+</sup> (53%–63%). Availability of the substrate also led to the ADP depletion in the suspension through oxidative phosphorylation in State 4 with further reduction of NAD<sup>+</sup> to the extent exceeding 99%. Utilization of ADP resulted in increased oxygen consumption and—very soon after the substrate addition—its depletion in the cuvette holding the mitochondrial suspension. At this period, defined as State 5, NADH was fully reduced.

It is important to note that the metabolic states of mitochondria in vivo are different in their levels of NADH. Accurate determination of the metabolic state of tissues in vivo requires the ability of changing various factors, as has been done by Chance and Williams (1955). In our in vivo experiments, the brain of the awaken rat was exposed to various conditions causing an oxidation or reduction of NADH (Mayevsky and Rogatsky 2007). We aimed to establish the range between the maximum increase and decrease in NADH level, as compared to the normoxic level. Our earlier studies (Mayevsky 1976) described the responses of the brain to an uncoupler, pentachlorophenol (PCP), injected into the lateral ventricle. In order to be certain that the NADH reduction was in fact due to PCP effect, the animal was exposed to an N<sub>2</sub> cycle every few minutes. After each N<sub>2</sub> cycle, which caused a large increase in NADH autofluorescence, the oxidation cycle was recorded as well. The results showed that PCP injection increases the range between maximal and minimal levels of NADH.

## 6.3 Methods

### 6.3.1 Principles and Technological Aspects of In Vivo NADH Monitoring

Two main approaches were historically applied in order to monitor NADH autofluorescence (Mayevsky and Rogatsky 2007). The earliest method was based on the measurements of the fluorescence spectrum of NADH (spectral approach). The second approach, established more than 50 years ago by Chance et al. (1962) and dominant for continuous measurements of NADH autofluorescence, relies on measuring the total fluorescence signal integrated into a single intensity using appropriate filters (integrated autofluorescence intensity approach). In addition to the measurement of the fluorescence signal, it is necessary to quantify the changes in tissue reflectance at the excitation wavelength. Tissue reflectance may introduce artifacts in NADH signal quantification and, therefore, affect its biological significance (Chance et al. 1973; Jöbsis et al. 1971; Mayevsky 1984).

As of today, two commercial devices for in vivo NADH monitoring were developed. In order to monitor NADH alone in animal models, a small compact system is available from Prizmatix Ltd. For human and animal studies, a multiparametric monitoring system was developed by CitiSense Ltd. This device is not available yet in the market. Monitoring of NADH redox state was performed by several types of fluorimeters that were developed in various laboratories around the world. We highlight in the following two major types of NADH fluorimeters.

### 6.3.2 Direct Current Fluorometer/Reflectometer

As an example of a typical direct current (DC) fluorometer/reflectometer, we present the one used in Mayevsky (1984), Mayevsky and Chance (1982), and Mayevsky et al. (1992). This device includes a metal

halide or mercury arc lamps as light source and a Y-shaped light guide (e.g., fiber bundle made of different numbers of fibers and diameter). Appropriate filters and photomultipliers (RCA 931B, Hamamatsu) are used to detect the reflectance and fluorescence signals (Figure 6.4a). Excitation light from the lamp passes through a 366 nm filter toward the tissue via a bundle of one arm of the Y-shaped light guide. The emitted light from the tissue is directed to the fluorometer through the second arm of the light guide and is then split at a 90:10 ratio with 90% of the light passing through a 450 nm filter and used as the fluorescence signal. The remaining 10% passes through the 366 nm filter and is used for the light reflectance measurements. This 90:10 ratio is empirical and provides adequate fluorescence and reflectance signals (Mayevsky et al. 1988). The fluorescence signal needs to be corrected by subtracting the reflectance signal from the fluorescence signal at a 1:1 ratio.

### 6.3.3 Time-Sharing Fluorometer/Reflectometer

The time-sharing fluorometer/reflectometer (TSFR) enables simultaneous monitoring of mitochondrial NADH redox and microcirculatory Hb oxygenation (Figure 6.4b). In this setup, NADH is monitored using the fluorometric technique described earlier, while two-wavelength reflectance allows for blood oxygenation measurements by comparing the reflectance of oxygenated ( $\text{HbO}_2$ ) and deoxygenated Hb—an approach introduced by Rampil et al. (1992). Although the absorption curves of  $\text{HbO}_2$  and Hb are different for the most of the spectra (Prahl 1999), they overlap at some wavelengths (called isosbestic points), where the molar extinction coefficients of both Hb species are the same (Figure 6.4c). Reflectance at an isosbestic wavelength is affected only by blood volume and light scattering. At non-isosbestic wavelengths, however, reflectance depends also on the  $\text{HbO}_2/\text{dHb}$  ratio. When subtracting the reflectance signals at these two wavelengths, the difference is considered as a qualitative representation of the Hb oxygenation levels in small blood vessels.

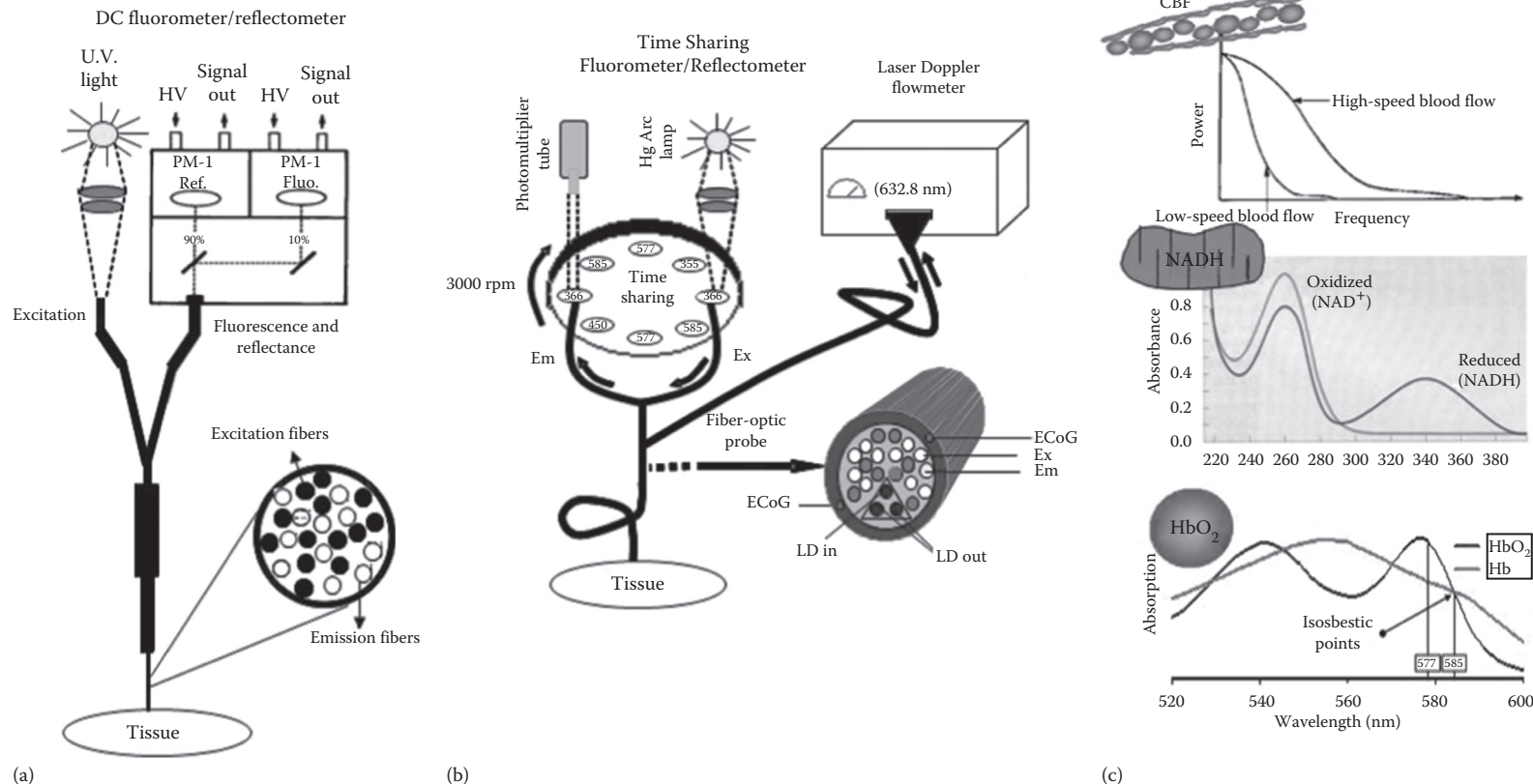
In these measurements, a mercury arc lamp can be used as the light source. Four sets of excitation/emission filter pairs determine the wavelengths for the measurement of (1) NADH fluorescence (366/450 nm), (2) Hb volumes at an isosbestic point (reflectance, 585/585 nm), (3) Hb oxygenation level (reflectance, 577/577 nm), and (4) correction of the NADH signal (reflectance, 366/366 nm) (Rampil et al. 1992). Filter sets are placed on the circumference of a wheel that rotates at approximately 3000 rpm. The light emitted from the tissue at four wavelengths is transferred to a photodetector, and the digitized signal is then recorded and stored in a special computerized system for further data analysis (LabVIEW A/D software, National Instruments). A laser Doppler flowmeter can also be coupled to the TSFR for measuring the microcirculatory blood flow. The optical fibers of the two devices can be constructed in a single probe, as seen in Figure 6.4b. This combination of laser Doppler flowmeter and TSFR enabled simultaneous monitoring of three parameters (Figure 6.4c).

### 6.3.4 Preparation of Various Organs for Measurements


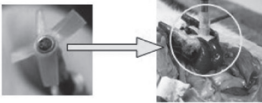
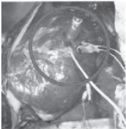
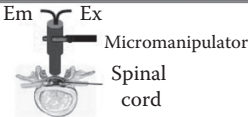
In order to measure NADH *in vivo*, it is necessary to have a constant, tight contact between the tip of the fiber-optic probe and the tissue under investigation. Since NADH autofluorescence signal provides relative units rather than absolute values, any disconnection between the probe and the tissue will require a new calibration after the relocation of the probe to a different region of the tissue. It is important to note that this is the crucial problem in any type of optical monitoring of blood-perfused organs due to the continuous changes in blood volume in response to pathophysiological events. In order to overcome these technical difficulties, we developed various protocols for NADH autofluorescence monitoring in various organs (Figure 6.5).

The simplest way to ensure tight contact between the probe and the tissue for brain investigation is shown in Figure 6.5a (Mayevsky and Chance 1975). In this protocol, a hole of an appropriate size is drilled in the bone and a light guide holder is fixed epidurally by dental acrylic cement





**FIGURE 6.4** (a) Schematic presentation of one unit of the DC fluorometer/reflectometer device for NADH fluorometry monitoring. HV, high voltage; PM, photomultiplier. (b) The time-sharing fluorometer-reflectometer device including the laser Doppler flowmeter and electrodes for electrocorticography (ECoG). Excitation and emission fibers for NADH and  $\text{HbO}_2$  monitoring, respectively; LD in- and out-optical fibers for blood flow monitoring. The numbers in the spinning disk refer to the wavelength filters. The tissue is connected to the monitoring system via a flexible fiber-optic probe. (c) The principles of monitoring the three parameters CBF, NADH, and  $\text{HbO}_2$  in the time-sharing device.

Probe to tissue connection		
Connection model	Connection model figure	Tissue/organ
A. Cementation		Brain
B. Adhesion		Soft tissue and visceral organs
C. Suturing		Heart and muscle
D. Micromanipulator		Spinal cord

**FIGURE 6.5** Various models for connecting the monitoring probe to the tissue and their application in the tissues and organs.

(Figure 6.5a, left). The fiber-optic probe is introduced into the holder to a preset depth and fixed with screws (Figure 6.5a, right).

The second approach is to use tissue adhesive (cyanoacrylate adhesive) at the fixation point of the probe on the tissue (Figure 6.5b). This approach is suitable for all soft tissues in the body, such as kidneys, small intestine, or liver. In this protocol, a small piece of parafilm paper is winded around the tip of the probe, leaving parafilm remainders that will be glued later on to the tissue (as seen in Figure 6.5b, left). In cases when the tissue under investigation is moving (e.g., beating heart), it is necessary to suture a light guide holder to the muscle tissue (Figure 6.5c). This will allow the contact between the fiber and the tissue to remain stable during data acquisition. We used this approach when a dog heart was monitored using an open-chest model (Kedem et al. 1981). For the spinal cord monitoring, a micromanipulator can be fixed to the animal operating table in order to hold the tip of the optical fiber in contact with the surface of the exposed spinal cord (Simonovich et al. 2008).

6.3.5 Calibration of the Monitored Signals

In order to monitor NADH in vivo in blood-perfused organs, it is necessary to record both fluorescence and reflectance. As mentioned earlier, the corrected NADH level is calculated by the subtraction of the reflectance changes from the fluorescence signal. It is important to note that the correction technology is dependent also on the system used. Therefore, any user that builds a new monitoring system should test and optimize the correction technology for the specific device. In our laboratory, we used the same type of fluorometers since 1972 until 2008. The principle of the calibration procedure was published in several papers (Osbakken and Mayevsky 1996; Osbakken et al. 1989).

6.4 Pitfalls and Remedies

Besides the redox state, other factors also affect the excitation and emission spectra of NADH and may be considered artifacts in fluorescence measurements. Since most fluorometers involve the measurement



of total backscattered light at the excitation wavelength, we discuss the artifacts in NADH autofluorescence detection as well as in tissue reflectance recording.

The following factors may affect the two measured signals, namely, reflectance, measured at 366 nm, and fluorescence, excited at 450 nm:

1. Tissue movement
2. Vascular and intravascular events, such as changes in Hb oxygenation level and blood volume due to the autoregulatory vasoconstriction under pathological conditions
3. Extracellular space events, such as volume changes or ion shifts between intra- and extracellular spaces
4. Intracellular space factors, such as  $O_2$  level, ATP turnover rate, substrate availability, and mitochondrial redox state

During the past 40 years, we have used fiber-optic surface fluorometry to monitor organs such as the brain and heart, which were exposed to various physiological conditions. Also, a good correlation was found between mitochondrial NADH and other physiological parameters monitored simultaneously (Mayevsky and Rogatsky 2007).

In the following, we briefly discuss the artifacts and their influence on the in vivo NADH measurements.

#### 6.4.1 Movement-Based Artifacts

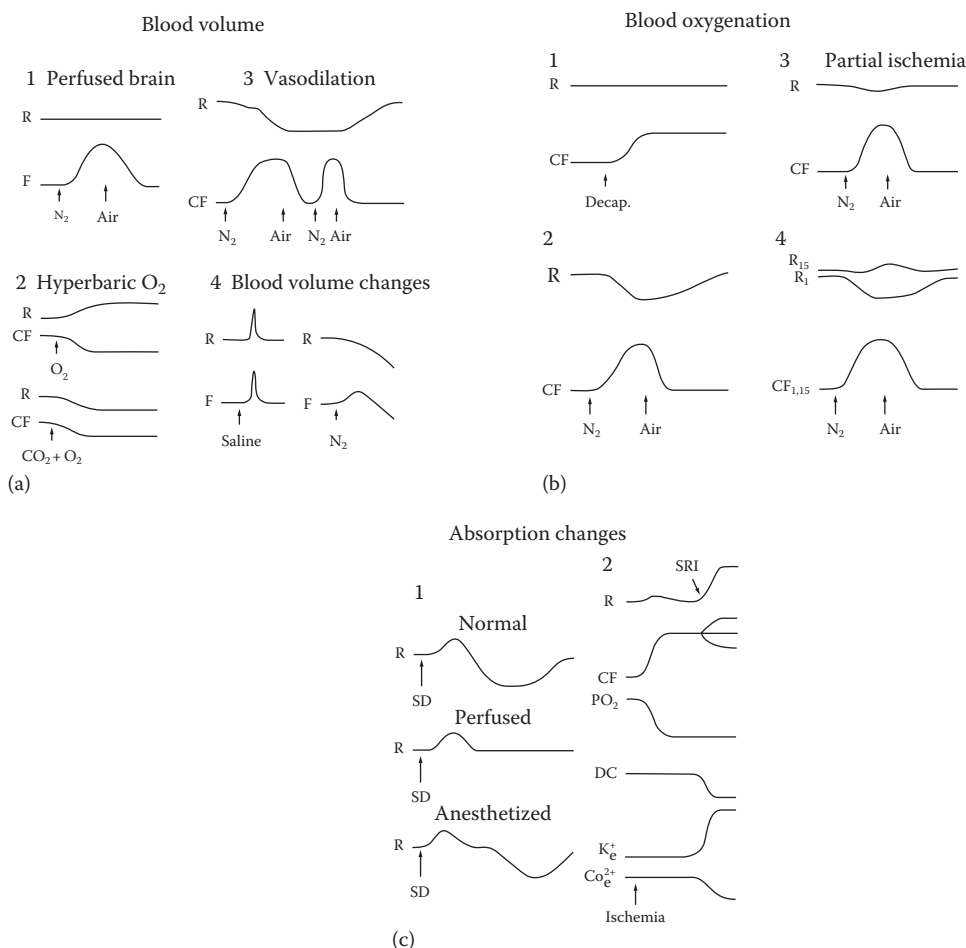
In order to obtain a good signal-to-noise ratio and perform reliable and reproducible measurements, good contact between the fibers and the tissue is required during the entire data acquisition period. Pressure on the tissue must be avoided, by using a special light guide holder connected to the tissue as shown in Figure 6.5a and described in Section 6.3.4. In brain measurements, even while the animal was undergoing hyperbaric convulsions or decapitation, only minor changes due to movement-based artifacts were observed, with a negligible effect on NADH autofluorescence. The same approach was applied previously to rats or cats using the “Ultrapac” optics for brain investigation (Jöbsis et al. 1971).

In order to avoid movement-based artifacts in monitoring human patients, we used various approaches. In the neurosurgical intensive care unit, for example, we used a metal holder that was screwed to the skull of comatose patients (Mayevsky et al. 1996). In the operating room, we used a floating light guide probe that was fixed to the head holder in neurosurgical procedures (Mayevsky et al. 1991, 1998, 1999) or a ring used to hold retractors during abdominal operations or kidney transplantations (Mayevsky et al. 2003).

#### 6.4.2 Vascular Events

Vascular events include changes in both blood volume in the microcirculation and blood oxygenation (namely, in the saturation level of  $HbO_2$ ). Vasodilatation of blood vessels will increase blood volume, while vasoconstriction will decrease blood volume (Figure 6.6a). These changes are the main source of artifacts in monitoring NADH autofluorescence in tissues (Mayevsky and Rogatsky 2007). Since Hb absorbs light strongly at various wavelengths, measurements of NADH autofluorescence are also affected by the level of hemoglobin oxygenation (Figure 6.6b). The influence of blood oxygenation transitions was found to be negligible: a decrease in absorption is compensated by an increase in the transmission of emitted fluorescence (Chance et al. 1973; Mayevsky 1992).

At monitoring a fluorochemically perfused brain preparation (Mayevsky et al. 1981), only negligible changes in reflectance were observed during the anoxic cycle. As shown in Figure 6.6a1, the uncorrected NADH autofluorescence and the corrected fluorescence (CF) had similar kinetics due to a stable reflectance trace. Furthermore, the CF response of the perfused brain to anoxia was similar to that of the



**FIGURE 6.6** (a) The effect of changes in blood volume, evaluated by the reflection, on NADH autofluorescence following anoxia (1, 3), hyperbaric oxygenation (2), and saline injection followed by anoxia (4). (b) The effect of blood oxygenation on the reflectance and NADH autofluorescence following decapitation (1) and anoxia (2–4) recorded with the standard DC fluorometer–reflectometer. (c) Effects of spreading depression (1) and ischemia (2) on the response measured from the brain. SD, spreading depression; SRI, secondary reflectance increase. (From Mayevsky, A. and Rogatsky, G.G., *Am. J. Physiol. Cell Physiol.*, 292(2), C615, 2007.)

blood-perfused brain in the same animal before the initiation of perfusion, as shown in Figure 6.6a3. The conclusion is that the blood in the brain affected the fluorescence signal but the reflectance correction approach provided reliable results.

### 6.4.3 Intra- and Extracellular Space Events

Another potential source of artifacts in NADH autofluorescence measurement is the change in the absorption properties of the tissue at the observation site during various physiological perturbations, such as local ischemia, hypoxia, or spreading depression in the brain. The effect of such fluctuations has mainly been recognized in brain studies.

Very little is known about this factor due to the inability to separate it from other artifacts affecting the recording of NADH fluorescence. For example, when severe ischemia or anoxia is induced for a

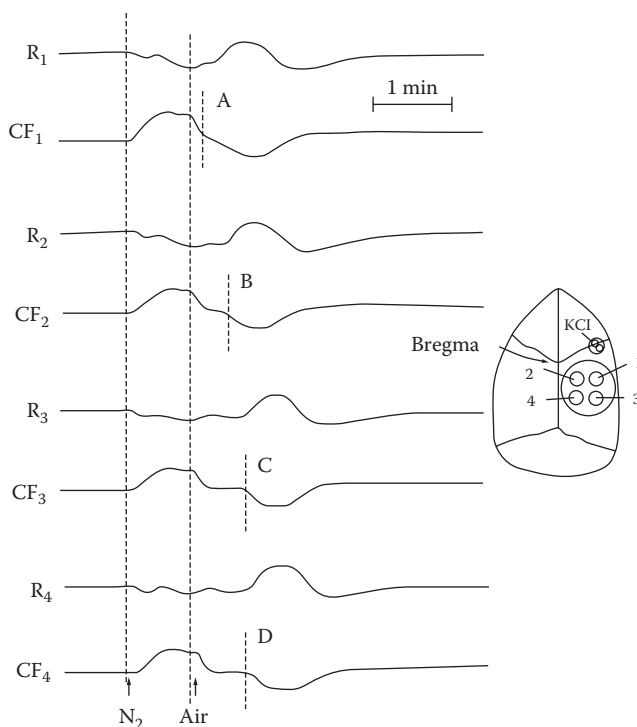
short time interval, the initial response of the fluorescence and reflectance will provide clear results. But if the event is longer, the reflectance change will be dramatically increasing due to shift of potassium ions to the extracellular space, as seen in Figure 6.6c2. Under these conditions, the correction technique for the fluorescence does not always work properly, and data will be distorted. It seems to us that under physiological or pathological conditions that involve both ions and water movement between the intracellular and the extracellular spaces, this factor may have a greater effect on NADH autofluorescence measurements.

## 6.5 Applications

This section contains typical results that demonstrate the methodological aspects described in the previous sections.

### 6.5.1 Effects of Anoxia on Brain

The effect of oxygen deprivation, shown in Figure 6.7, was recorded from the brain of an anesthetized rat. In this animal, NADH was monitored in four sites on the right hemisphere. Four light guides connected to the four-channel DC fluorometer/reflectometer were used for this purpose. Brain exposure to



**FIGURE 6.7** Metabolic responses of a gerbil brain to anoxia as monitored in four different locations in one hemisphere. The schematic drawing shows the location of the four light guides on the surface of the parietal cortex. The letters A–D mark the point in which spreading depression was observed, demonstrating the propagation of the wave through the hemisphere, as observed also by the increasing distance between the time in which recovery from the anoxic episode was achieved and the point in which SD started. (From Mayevsky, A. and Chance, B., *Science*, 217(4559), 537, 1982.)

anoxia (ventilation with nitrogen) led to a very similar increase in corrected NADH signal at all four points. The NADH reached the baseline immediately after the exposure to air. A wave of cortical spreading depression was developed and led to an oxidation of NADH. This wave propagated from site 1 to site 4, as seen in the location of lines A to D (Mayevsky and Chance 1982).

Application of the TSFR is demonstrated in [Figure 6.8](#). In this system, the laser Doppler flowmeter was added in order to monitor cerebral blood flow (CBF) (Meirovithz et al. 2007). Exposure of the rat to anoxia, similar to the previous experiment, led to a reduction of the HbO<sub>2</sub> and thereby reduced the supply of oxygen to the brain, as revealed by the increase in NADH signal. The microcirculatory blood flow started with a small decrease, followed by a large increase—hyperemia. The reflectance at 366 nm decreased due to a large increase in blood volume induced by the lack of oxygen. The results presented in [Figure 6.8](#) are an average from a group of rats. Statistical analysis indicated that immediately after 100% N<sub>2</sub> inhalation, CBF, reflectance, and HbO<sub>2</sub> levels decreased significantly ( $p < 0.01$ ,  $p < 0.001$ , and  $p < 0.001$ , respectively), while mitochondrial NADH significantly increased by about 35% ( $p < 0.001$ ). The maximum decrease in HbO<sub>2</sub> and increase in NADH during the anoxia period were calculated from all experimental groups and were  $25.14\% \pm 1.39\%$  and  $42.66\% \pm 1.12\%$ , respectively. Within 1 min after returning to spontaneous air breathing led to a significant ( $p < 0.001$ ) increase (about 75%) in CBF with further gradual return to the basal levels. Reflectance, NADH redox state, and HbO<sub>2</sub> fully recovered within a few minutes (Meirovithz et al. 2007).

### 6.5.2 Effects of Adrenaline on the Small Intestine and the Brain

Influence of adrenaline was measured by simultaneous recording from brain and small intestine with two channels of a DC fluorometer/reflectometer and two channels of a laser Doppler flowmeter ([Figure 6.9](#)). The mean arterial pressure (MAP) was measured from the tail artery. Adrenaline administration led to large increase in blood pressure due to the sympathetic stimulation and vasoconstriction of the microcirculation in the small intestine, as indicated by the large decrease in intestinal tissue blood flow (TBF) with concurrent increase of blood flow in the brain due to the sparing effect. The change in the perfusion of both organs was also indicated by the NADH responses. In the brain, the NADH level slightly decreased, while the mitochondrial function in the small intestine was inhibited. The corresponding NADH level, measured by its autofluorescence, exhibited a significant increase (Tolmasov et al. 2007).

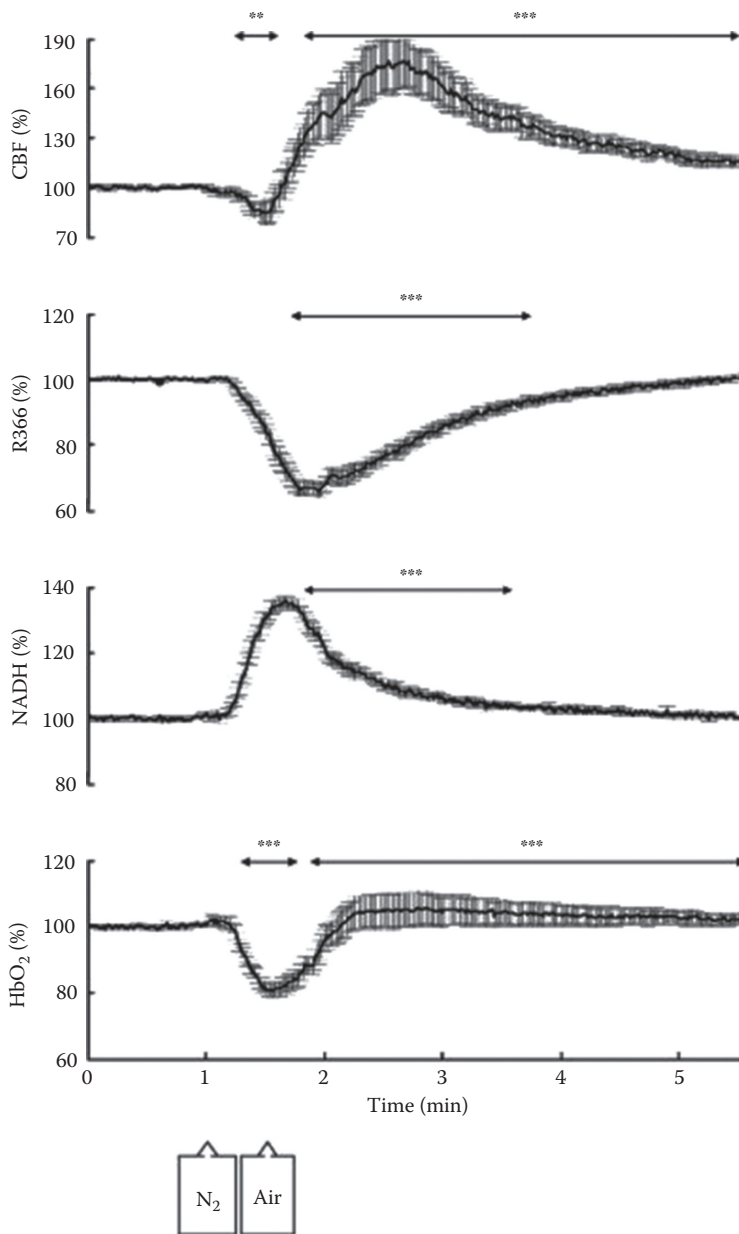
### 6.5.3 Effect of Oxygen Deprivation on the Heart

The response of a dog heart to the lack of O<sub>2</sub> was monitored in vivo by a fiber-optic DC fluorometer-reflectometer. The dog was exposed to a short ([Figure 6.10a](#)) and long ([Figure 6.10b](#)) anoxia period. In both anoxic episodes, the NADH level was elevated significantly. In the second longer anoxia ([Figure 6.10b](#)), the heart went into fibrillation and the dog died.

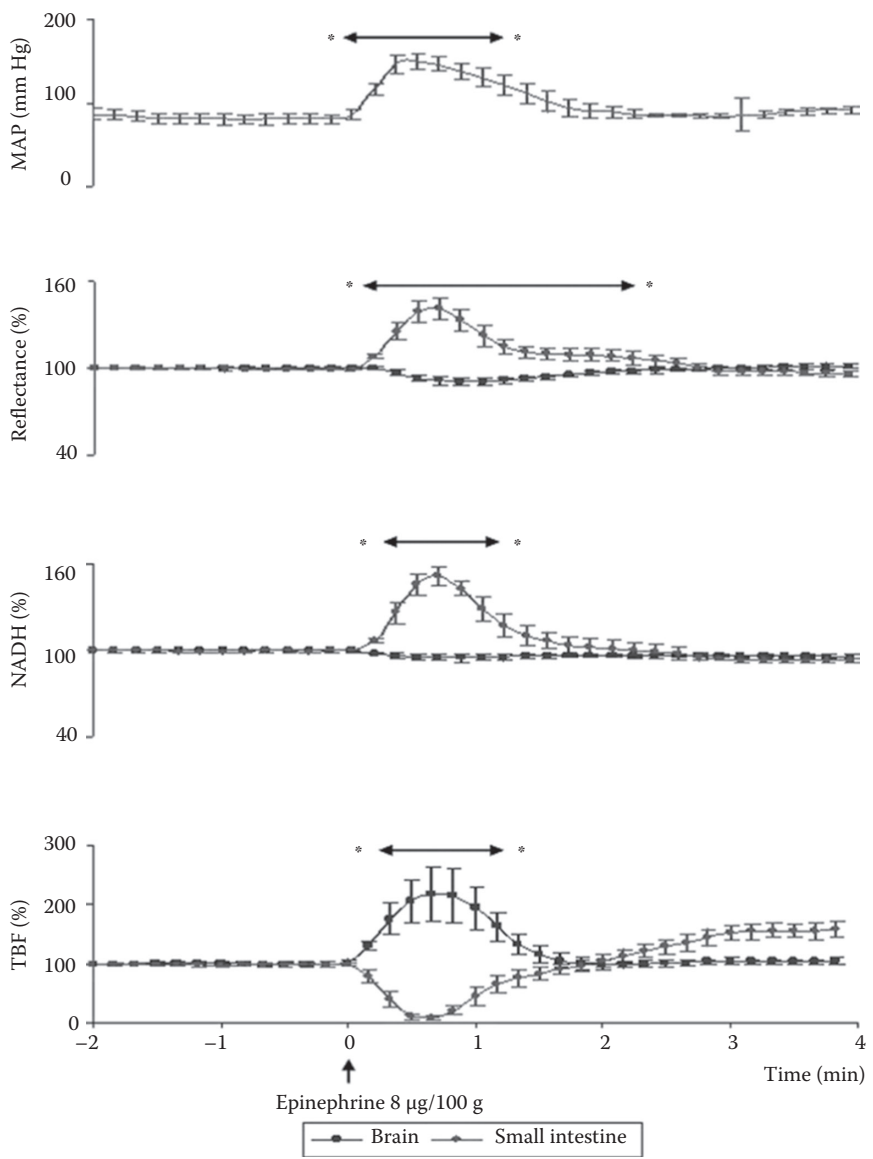
The effect of hypoxia in the same dog model is shown in [Figure 6.10c](#). The dog was artificially ventilated during the entire experiment. Hypoxia was induced by lowering the oxygen level in the respiration mixture. Decrease in inspired oxygen led to an increase in NADH redox state.

The same type of dog model was used in studying the effects of local ischemia (Osbakken and Mayevsky 1996). The left anterior descending artery was isolated for later occlusion. In [Figure 6.10d](#), the coronary artery occlusion led to a dramatic drop in blood flow and a very large increase in NADH, while the change in the reflectance signal was very small. The changes in blood flow measured by a laser Doppler flowmeter were typical for an ischemic event (Osbakken and Mayevsky 1996).

The effect of hypopnea in the dog heart model is shown in [Figure 6.10e](#). Under this condition, the ventilation of the lungs was not optimal and the elevated carbon dioxide in the blood led to an



**FIGURE 6.8** The effect of anoxia (100% N<sub>2</sub>) on CBF, reflectance (R366), mitochondrial NADH redox state (NADH), and hemoglobin oxygen saturation (HbO<sub>2</sub>). Values are shown as mean percent values  $\pm$  SE. \*\* $p < 0.01$ , \*\*\* $p < 0.001$  range of time showing significant differences found by ANOVA repeated measures. Please see Meirovithz et al. (2007).



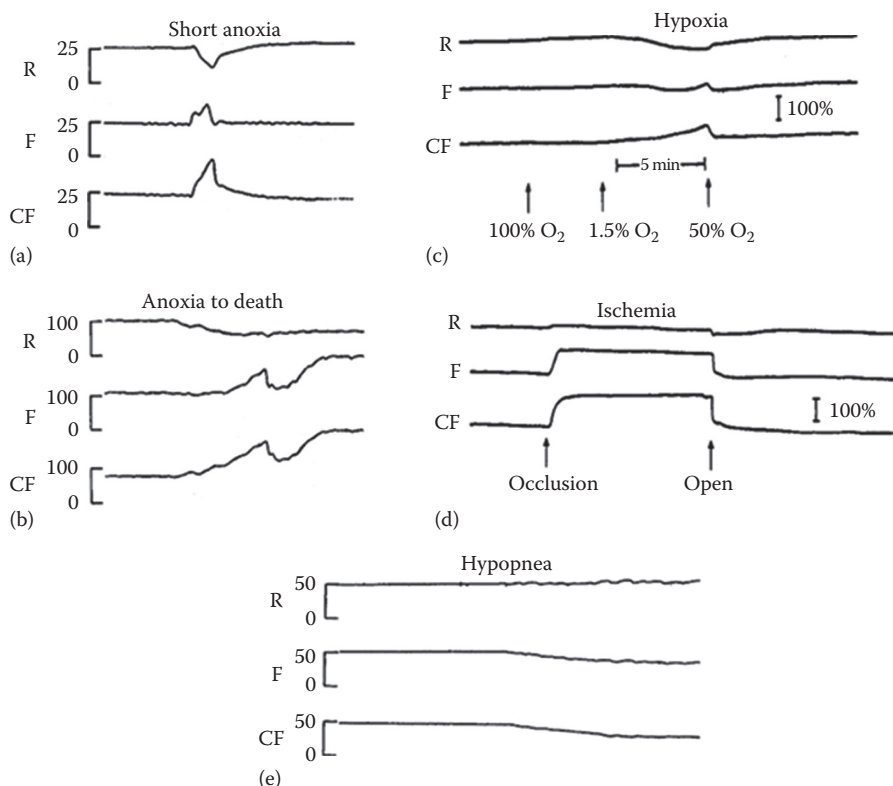
**FIGURE 6.9** The responses of the brain and small intestine to epinephrine injection (8 µg/100 g IV). Arrows represent the period of time in which the differences between the two organs were significant. (N=9) \*p<0.05.

increase in blood flow to the heart (data not shown here) and to the oxidation of NADH (Osbakken and Mayevsky 1996).

6.5.4 Responses of the Spinal Cord to Ischemia

Spinal cord ischemia was induced by transient occlusion of the abdominal aorta distal to the left kidney (Figure 6.11). This operation led to a dramatic decrease in spinal cord blood flow to 19.9%±6.1% (not shown). This was correlated with a significant rise of the detected signals: by 25%±9.3% for tissue





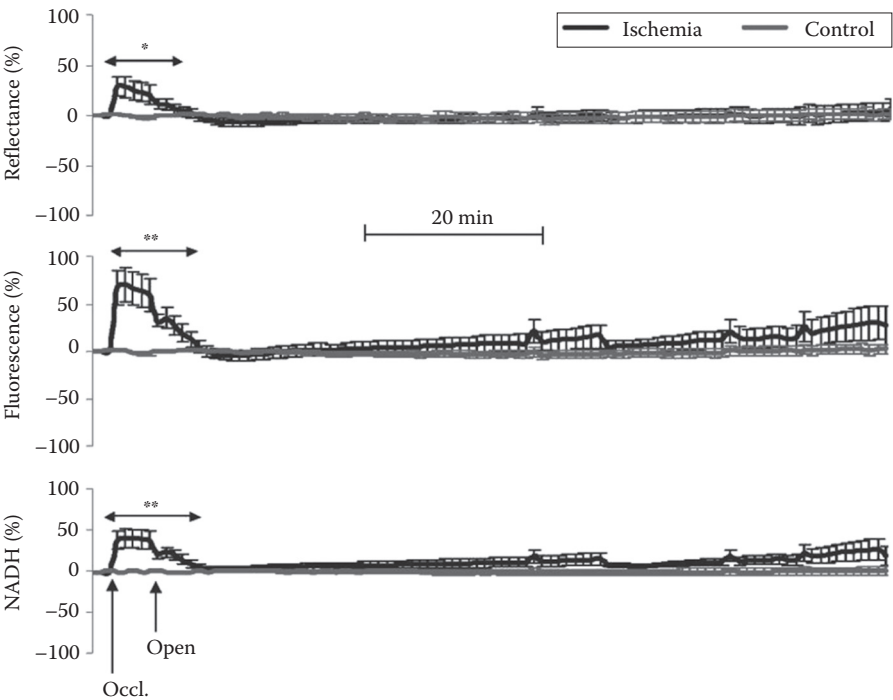
**FIGURE 6.10** Responses of the canine heart to various perturbations affecting oxygen supply to the beating heart. Five perturbations are presented including (a and b) short and long anoxia, (c) hypoxia, (d) ischemia, and (e) hypopnea. Please see Osbakken and Mayevsky (1996).

reflectance, by  $70\% \pm 17.2\%$  for tissue autofluorescence, and by  $39\% \pm 11.1\%$  for the corrected NADH levels. These changes were significantly higher than the basal level of each parameter and greater than the control levels ( $p < 0.01$ ).

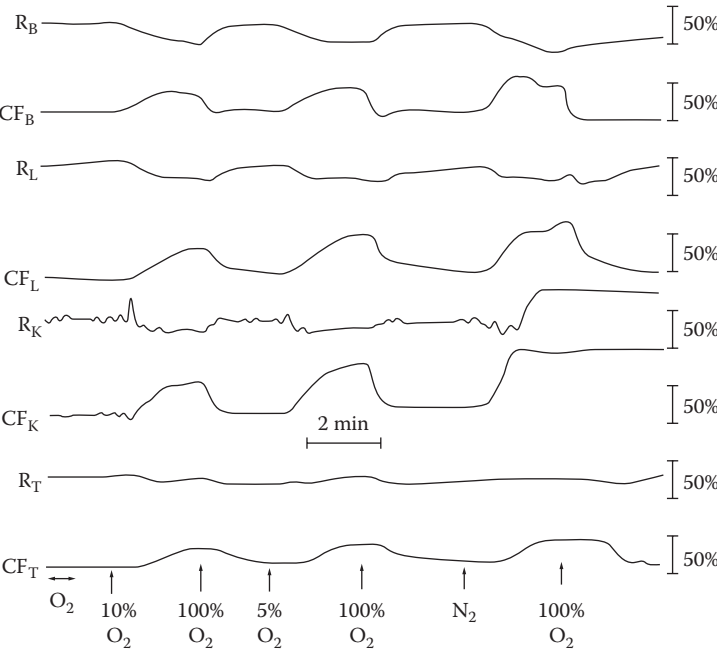
With the release of the occlusion, the increase in the spinal CBF reached hyperemia levels ( $p < 0.01$ ) within the first 10 min of the reperfusion. The reflectance, fluorescence, and NADH signal also returned gradually to their initial levels. Through the rest of the monitoring period (1.5 h), all parameters stayed stable (Simonovich et al. 2008).

### 6.5.5 Multiorgan Responses to Hypoxia

Figure 6.12 demonstrates the responses of four different organs to systemic hypoxia that were induced by lowered oxygen level in the air mix supplied for rat ventilation. Four organs were monitored by the multichannel fluorometer/reflectometer: brain, liver, a kidney, and a testis. Levels of oxygen were varied from high (100%) to lower levels of 10% and 5%; pure nitrogen was used to model anoxia. Elevation of NADH levels due to the limited oxygen was proportional to the severity of hypoxia. The responses of all four organs to the systemic hypoxia were similar; however, the amplitude of changes was bigger in the brain, liver, and kidney as compared with the testis, which has low metabolic rate (Mayevsky and Rogatsky 2007).



**FIGURE 6.11** The responses of the spinal cord to 5 min of ischemia induced by the occlusion of the abdominal aorta (ischemia) versus continuous monitoring (control). Please see Simonovich et al. (2008).



**FIGURE 6.12** Typical responses of the tissue reflectance (R) and NADH redox state (CF) simultaneously monitored in four organs to various oxygen concentrations and to anoxia: brain (B), liver (L), kidney (K), and testis (T) (see Mayevsky and Chance 1982).

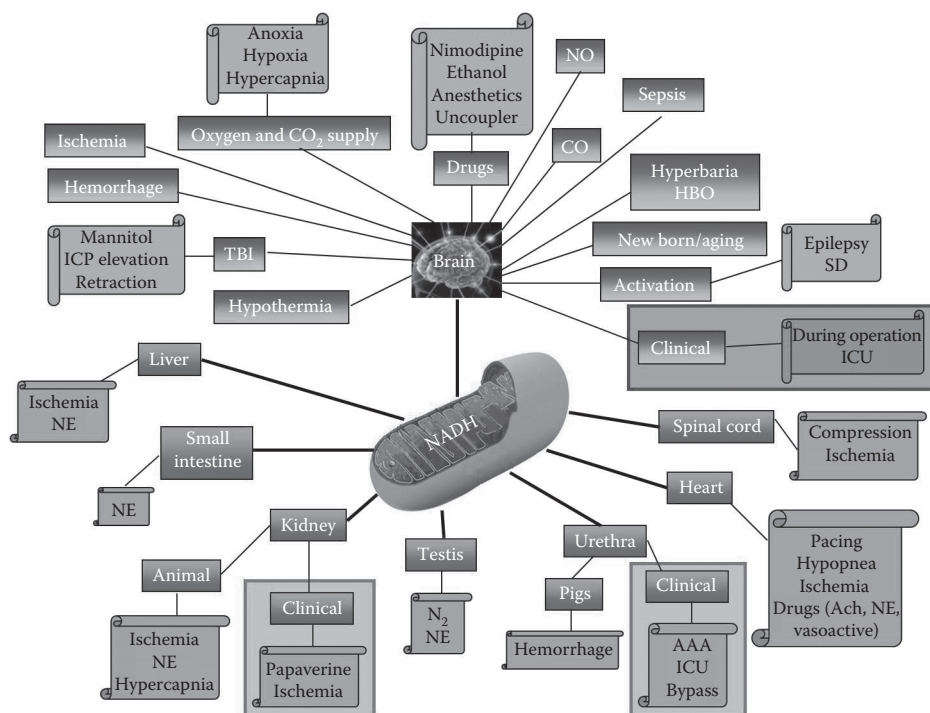
## 6.6 Summary

Development of biophotonics in the last 50 years opened up the possibility to monitor energy metabolism of tissues in intact in vivo organs. The main problem in monitoring mitochondrial signals in blood-perfused organs is the hemodynamic artifacts, which require correction in real time for physiological significance.

We found that only NADH autofluorescence could provide relatively a “clean” signal after correcting the hemodynamic-based artifacts. As presented in Figure 6.13, we have applied the multiparametric monitoring technique through the years to various organs and in response to various perturbations under in vivo conditions.

Among those organs that we investigated are brain, spinal cord, kidneys, liver, heart, small intestine, urethra, and testes. The conditions that were tested included models in which oxygen or blood supply is decreased (anoxia, hypoxia, ischemia, and hemorrhage) or increased (hyperoxia and hyperbaria). We also tested the effects of various drugs (norepinephrine [NE], mannitol, etc.) on the various organs. Models of brain activation, such as spreading depression and epilepsy, were also studied. We also run several clinical studies using patients hospitalized in the intensive care units and in operation rooms.

We used the NADH monitoring technology in patients and found results that are basically the same as was found in animal models. In most cases, we combined more physiological parameters to the NADH, and the results showed clinical significance. Two reviews were published recently and the reader can find more details there (Mayevsky and Barbiro-Michaely 2013a,b; Mayevsky et al. 2011).



**FIGURE 6.13** Summary of 40 years of mitochondrial NADH monitoring in vivo. The monitored organs and perturbations measured by Mayevsky and his collaborators in experimental animals as well as in patients are presented (for details, see Mayevsky and Rogatsky 2007).

## References

- Chance, B., P. Cohen, F. Jöbsis, and B. Schoener. 1962. Intracellular oxidation-reduction states in vivo the microfluorometry of pyridine nucleotide gives a continuous measurement of the oxidation state. *Science* 137(3529): 499–508.
- Chance, B., N. Oshino, T. Sugano, and A. Mayevsky. 1973. Basic principles of tissue oxygen determination from mitochondrial signals. In: *Oxygen Transport to Tissue: Instrumentation, Methods, and Physiology*, H. I. Bicher and D. F. Bruley (eds.), Vol. 37A of *Advances in Experimental Medicine and Biology*, I. R. Cohen, A. Lajtha, J. D. Lambris, and R. Paoletti (eds.), pp. 277–292. New York: Springer.
- Chance, B. and G. R. Williams. 1955. Respiratory enzymes in oxidative phosphorylation. III. The steady state. *Journal of Biological Chemistry* 217(1): 409–427.
- Harden, A. and W. J. Young. 1906. The alcoholic ferment of yeast-juice. *Proceedings of the Royal Society of London. Series B, Containing Papers of a Biological Character* 77(519): 405–420.
- Jöbsis, F. F., M. O'Connor, A. Vitale, and H. Vreman. 1971. Intracellular redox changes in functioning cerebral cortex. I. Metabolic effects of epileptiform activity. *Journal of Neurophysiology* 34(5): 735–749.
- Kedem, J., A. Mayevsky, J. Sonn, and B.-A. Acad. 1981. An experimental approach for evaluation of the  $O_2$  balance in local myocardial regions in vivo. *Quarterly Journal of Experimental Physiology* 66(4): 501–514.
- Mayevsky, A. 1976. Brain energy metabolism of the conscious rat exposed to various physiological and pathological situations. *Brain Research* 113(2): 327–338.
- Mayevsky, A. 1984. Brain NADH redox state monitored in vivo by fiber optic surface fluorometry. *Brain Research Reviews* 7(1): 49–68.
- Mayevsky, A. 1992. Interrelation between intracellular redox state and ion homeostasis in the brain in vivo. In: *Quantitative Spectroscopy in Tissues*, K. Frank and M. Kessler (eds.), pp. 155–168. Frankfurt am Main, Germany: PMI Verlagsguppe.
- Mayevsky, A. and E. Barbiro-Michaely. 2013a. Shedding light on mitochondrial function by real time monitoring of NADH fluorescence: I. Basic methodology and animal studies. *Journal of Clinical Monitoring and Computing* 27(1): 1–34.
- Mayevsky, A. and E. Barbiro-Michaely. 2013b. Shedding light on mitochondrial function by real time monitoring of NADH fluorescence. II. Human studies. *Journal of Clinical Monitoring and Computing* 27(1): 125–145.
- Mayevsky, A. and B. Chance. 1975. Metabolic responses of the awake cerebral cortex to anoxia, hypoxia, spreading depression and epileptiform activity. *Brain Research* 98(1): 149–165.
- Mayevsky, A. and B. Chance. 1982. Intracellular oxidation reduction state measured in situ by a multi-channel fiber-optic-surface fluorometer. *Science* 217(4559): 537–540.
- Mayevsky, A., A. Doron, T. Manor, S. Meilin, N. Zarchin, and G. E. Ouaknine. 1996. Cortical spreading depression recorded from the human brain using a multiparametric monitoring system. *Brain Research* 740(1): 268–274.
- Mayevsky, A., A. Doron, S. Meilin, T. Manor, E. Ornstein, and G. E. Ouaknine. 1999. Brain viability and function analyzer: Multiparametric real-time monitoring in neurosurgical patients. In: *Neuromonitoring in Brain Injury*, R. Bullock, A. Marmarou, B. Alessandri, and J. Watson (eds.), Vol. 75 of *Acta Neurochirurgica Supplements*, H.-J. Steiger (ed.), pp. 63–66. New York: Springer.
- Mayevsky, A., E. S. Flamm, W. Pennie, and B. Chance. 1991. Fiber optic based multiprobe system for intra-operative monitoring of brain functions. *Proceedings of SPIE* 1431: 303.
- Mayevsky, A., K. Frank, M. Muck, S. Nioka, M. Kessler, and B. Chance. 1992. Multiparametric evaluation of brain functions in the Mongolian gerbil in vivo. *Journal of Basic Clinical Physiology and Pharmacology* 3(4): 323–342.

- Mayevsky, A., T. Manor, S. Meilin, A. Doron, and G. E. Ouaknine. 1998. Real-time multiparametric monitoring of the injured human cerebral cortex—A new approach. In: *Intracranial Pressure and Neuromonitoring in Brain Injury*, A. Marmarou et al. (eds.), Vol. 71 of Acta Neurochirurgica Supplements, H.-J. Steiger (ed.), pp. 78–81. New York: Springer.
- Mayevsky, A., I. Mizawa, and H. A. Sloviter. 1981. Surface fluorometry and electrical activity of the isolated rat brain perfused with artificial blood. *Neurological Research* 3(4): 307–316.
- Mayevsky, A., S. Nioka, and B. Chance. 1988. Fiber optic surface fluorometry/reflectometry and <sup>31</sup>P-NMR for monitoring the intracellular energy state in vivo. In: *Oxygen Transport to Tissue X*, M. Mochizuki (ed.), Vol. 215 of Advances in Experimental Medicine and Biology, I. R. Cohen, A. Lajtha, J. D. Lambiris, and R. Paoletti (eds.), pp. 365–374. New York: Springer.
- Mayevsky, A. and G. G. Rogatsky. 2007. Mitochondrial function in vivo evaluated by NADH fluorescence: From animal models to human studies. *American Journal of Physiology. Cell Physiology* 292(2): C615–C640.
- Mayevsky, A., J. Sonn, M. Luger-Hamer, and R. Nakache. 2003. Real-time assessment of organ vitality during the transplantation procedure. *Transplantation Reviews* 17(2): 96–116.
- Mayevsky, A., R. Walden, E. Pewzner et al. 2011. Mitochondrial function and tissue vitality: Bench-to-bedside real-time optical monitoring system. *Journal of Biomedical Optics* 16(6): 067004.
- Meiurovithz, E., J. Sonn, and A. Mayevsky. 2007. Effect of hyperbaric oxygenation on brain hemodynamics, hemoglobin oxygenation and mitochondrial NADH. *Brain Research Reviews* 54(2): 294–304.
- Osbakken, M. and A. Mayevsky. 1996. Multiparameter monitoring and analysis of in vivo ischemic and hypoxic heart. *Journal of Basic and Clinical Physiology and Pharmacology* 7(2): 97–114.
- Osbakken, M., A. Mayevsky, I. Ponomarenko, D. Zhang, C. Duska, and B. Chance. 1989. Combined in vivo NADH fluorescence and <sup>31</sup>P NMR to evaluate myocardial oxidative phosphorylation. *Journal of Applied Cardiology* 4(5): 305–313.
- Prahl, S. 1999. Optical absorption of hemoglobin. <http://omlc.ogi.edu/spectra/hemoglobin/>. Accessed January 10, 2014.
- Rampil, I. J., L. Litt, and A. Mayevsky. 1992. Correlated, simultaneous, multiple-wavelength optical monitoring in vivo of localized cerebrocortical NADH and brain microvessel hemoglobin oxygen saturation. *Journal of Clinical Monitoring* 8(3): 216–225.
- Simonovich, M., E. Barbiro-Michaely, and A. Mayevsky. 2008. Real-time monitoring of mitochondrial NADH and microcirculatory blood flow in the spinal cord. *Spine* 33(23): 2495–2502.
- Tolmasov, M., E. Barbiro-Michaely, and A. Mayevsky. 2007. Simultaneously multiparametric spectroscopic monitoring of tissue viability in the brain and small intestine. *Proceedings of SPIE* 6434: 64341N.

